Polymer Chemistry

Accepted Manuscript

ROYAL SOCIETY OF CHEMISTRY

www.rsc.org/polymers

Cite this: DOI: 10.1039/c0xx00000x

www.rsc.org/xxxxxx

ARTICLE TYPE

Enhanced actuation response of ionic polymer-metal composite actuator based on sulfonated polyphenylsulfone

Yongjun Tang, Chao Chen, Yun Sheng Ye, Zhigang Xue,* Xingping Zhou and Xiaolin Xie*

Received (in XXX, XXX) Xth XXXXXXXXX 200X, Accepted Xth XXXXXXXXX 200X

DOI: 10.1039/b000000x

The sulfonated polyphenylsulfone (SPPSU) membranes with different degrees of sulfonation (DS) were prepared for fabricating low-cost and high-performance ionic polymer-metal composite (IPMC) actuators. The properties of SPPSU ion exchange membranes and the electromechanical performance of resulting SPPSU actuators can be manipulated by controlling their DS. As the DS of SPPSU membranes increases, their ion exchange capacity (IEC), water uptake and ion conductivity increase accordingly, whereas the hydrated mechanical properties (strength and modulus) decrease. The SPPSU membrane with the highest DS (SPPSU4) shows much higher IEC and water uptake, and slightly lower ion conductivity than those of the traditional Nafion membrane. Among the prepared IPMC actuators, the SPPSU4 actuator performs the best in the bending deformation under the electric stimulus. The maximum bending strain (MBS) of SPPSU4 actuator is comparable to that of Nafion actuator coupled with several times faster bending response at 3 V DC voltage. Compared with Nafion system, the SPPSU4 actuator increases approximately twice at MBS under sinusoidal voltage of 3 V at 1 Hz. These greatly enhanced actuation performance indicates the SPPSU is a candidate to substitute Nafion in the field of IPMC actuator.

Introduction

Ionic polymer-metal composite (IPMC) is one of the most promising elctroactive polymer (EAP) materials, which has attracted much attention owing to its unique actuation and sensing capabilities.[1-4] Compared with other types of EAP-based actuators, IPMC actuator exhibits a large bending strain (displacement) under a low applied voltage (1-3 V). Besides, IPMC has many attractive features including: flexibility, light weight, easy miniaturization, low power consumption, high force/weight ratio, and rapid response. These excellent characteristics make IPMC be attractive for potential applications in soft actuators, soft sensors and artificial muscles.[5-7] The IPMC has a sandwich-like configuration, typically consisting of an ion exchange membrane covered by two layers of thin metal electrodes (e.g. Pt or Au) on both surfaces through the impregnation-reduction method. When a hydrated cantilever strip of IPMC is subjected to a low driving voltage, the IPMC undergoes a fast bending deformation toward the anode. Conversely, charge in term of voltage or current will be produced between two sides of IPMC if the IPMC is stimulated by mechanical bending deformation. The above-mentioned two unique functions of IPMC are considered to be its actuation and sensing capability, respectively. In general, the IPMC's actuation mechanism is thought to be primarily due to asymmetric swelling of IPMC strip, namely expansion of the cathode side and contraction of the anode, resulting from the combined effects of cation's migration and water molecule's electro-osmosis toward the cathode under the electric field.[4]

The electromechanical performance (strain or force) of IPMC actuator mainly depends on the kind of cation, the amount of absorbed solvent, the quality of plated metal electrode, and the property and dimension of ion exchange membrane or polyelectrolyte membrane.[8-10] The composition, nature and morphology of ion exchange membrane which is one of the most crucial components of IPMC actuator can severely affect and modulate the performance of the resulting IPMC actuator. The most widely used polyelectrolyte membrane in IPMC actuator is Nafion (Dupont), which has some advantages, such as commercially availability, proper mechanical robustness, excellent chemical stability and high proton conductivity. Although the Nafion-based IPMC actuator has demonstrated good actuation performances (large strain or displacement, and quick response) under electric voltage stimulus, there are still some inherent drawbacks which limit its practical applications, such as high cost, environment-unfriendliness, low water-retention capability, low actuation force, back-relaxation under direct current (DC) voltage, and unalterable physical properties (e.g. fixed ion exchange capacity and proton conductivity). Therefore, many easily synthesizable and inexpensive polyelectrolyte membranes have been used in IPMC actuators to replace Nafion membranes.[5-7]

Inspired from the chemical structure of Nafion, Jeong and Kim et al. prepared the first IPMC actuator using fluorinated acrylic copolymer membranes instead of Nafion.[11,12] No back relaxation was observed for all actuators during the DC test. However, the high voltage (3-8 V) was needed for the actuation. Moreover, fluorinated monomers were not cheap and not environmentally–

friendly. Since then, some industrial-grade polymers, such as nonfluorinated hydrocarbon polymers and a few fluorinated polymers, have been used to develop novel IPMC actuators after simple chemical modification. For polymers, sulfonation and carboxylic acidification are two major methods of chemical modification in order to transform ordinary polymers into polyelectrolytes (ion-exchange resins). Sulfonated polymers used in IPMC actuators included: radiation-grafted fluoropolymers,[13-15] sulfonated aromatic block polymers,[16-22] sulfonated random copolymers,[23-27] sulfonated condensation polymers,[28-33] sulfonated semi-interpenetrating networks,[34-36] sulfonated homopolymers and their blends or composites.[37-44] Meanwhile, relatively few carboxylated polymers derived from radical copolymerization were also employed to prepare IPMC actuators, e.g. fluorinated acrylic copolymers[11,12,45] and acrylic acid copolymers.[26,27] Very recently, Oh, Kim, and Asaka et al. reported a review paper about various types of novel hydrocarbon-backbone ionic polymer membranes used in the IPMC application.[7] As stated above, many efforts have been undertaken to develop new, easily synthesized, cost-effective and high-performance ionic membranes as alternatives of the traditional Nafion membrane for IPMC actuators, and improve their electromechanical performance. However, so far, the efforts of replacement have been only partially successful. Thus, it is still required to continue to seek new ionic polymers as alternatives used in high-performance IPMC actuators.

sulfonated polyphenylsulfone (SPPSU) which has its excellent mechanical and chemical stablility, good film-forming capacity, high hydrophilicity, high ionic conductivity and low price has been successfully used in some fields, such as fuel cells[46,47] and reverse osmosis membranes for water purification.[48] However, to the best of my knowledge, the use of SPPSU as ion exchange membrane for IPMC application has been not appeared so far. Furthermore, only very few studies have been concentrated on the effect of DS or IEC of polyelectrolyte membranes on the electromechanical response for the corresponding IPMC actuators.[13-15,37] In this study, SPPSU was synthesized through post-sulfonation method with chlorosulfonic acid (CSA) as sulfonating reagent, and used to prepare IPMC actuator for the first time by solution-casting and subsequent chemical plating of metal electrodes. Four kinds of SPPSU membranes with different degrees of sulfonation (DS) were synthesized, and their ion exchange capacity, water uptake, ionic conductivity, mechanical properties were studied. The electromechanical performances of the as-prepared IPMC actuators in term of bending displacement under DC and AC voltages were investigated according to their DS and compared with the Nafion counterpart.

Experimental

Materials

Polyphenylsulfone (PPSU, Radel R-5500, M_w = 60,700) was purchased from Solvary Company (USA), and vacuum dried at 100 °C overnight prior to use. Tetraamineplatinum chloride hydrate ($[Pt(NH_3)_4]Cl_2$) was provided by Aladdin Industrial Inc., China. Nafion 117 membranes are from Dupont (USA). All other chemicals were supplied from Sinopharm Chemical Reagent Co., Ltd (China) and used as received without further purification.

Preparations of sulfonated polyphenylsulfone (SPPSU) and SPPSU membranes

The synthesis of SPPSU was carried out in dichloromethane (CH_2Cl_2) solvent using chlorosulfonic acid (CSA) as sulfonation agent at 0 °C following the procedure described by Hartmann-Thompson et. al.[49] Typically, the dried PPSU (20 g) was completely dissolved in 200 mL of CH_2Cl_2 for 2 h at room temperature. Then, a certain volume of CSA was added to another 100 mL of ice-cooled CH_2Cl_2. The mixture solution was added slowly to the aforementioned PPSU solution immediately under vigorous stirring within 25 minutes, and the reaction continued for further 5 minutes at 0 °C. Finally, the SPPSU was obtained by pouring all the reaction solution into a large amount of frozen ice. The product was filtered and washed with DI water repeatedly until a neutral pH level. The SPPSU samples were dried at 60 °C for 48 h, and followed by drying at 100 °C under vacuum for 72 h.

The SPPSU membranes were prepared by the solution casting method. Firstly, the SPPSU was dissolved in *N*,*N*-dimethylacetamide (DMAc) at 60 °C to make a 35 wt% homogeneous solution. The solution was then cast onto a clean glass plate and spread thoroughly by using a doctor blade with 600-700 μm gap. The solvent was removed by first air drying at 35 °C for 12 h, then drying at 65 °C and 85 °C for 2 h respectively, and finally followed by further drying at 135 °C for 3h. The resulting membranes were peeled off from the glass plate. The thickness of dried SPPUS membranes was measured in the range of 100-120 μm with a digital micrometer. According to different volumes of CSA used in sulfonation reactions, the degree of sulfonation (DS) of these four SPPSU membranes were 91.1%, 98.5%, 101.2%, 108.7%, respectively. Following the increasing order of DS, SPPSU membranes with different DS were named sequentially as SPPSU1, SPPSU2, SPPSU3 and SPPSU4, respectively.

Preparation of IPMC actuators

Electroactive IPMC actuators were fabricated using the SPPSU membranes by an electroless plating method (namely, impregnation-reduction) as described in Refs.[50,51] The whole process of plating Platinum consisted of two reduction steps: primary reduction by using a strong reductant ($NaBH_4$) and surface or secondary reduction by using the combination of two weak reductants (NH_2NH_2 and $NH_2OH{\cdot}HCl$). The SPPSU membranes were initially roughened by metallographic abrasive paper (1200 mesh) in order to increase the surface area, followed by water-washing, soaking in HCl aqueous solution (1 M) and rinsing with DI water in sequence. The pretreated membrane (1cm × 5 cm) was immersed in 120 mL of aqueous $[Pt(NH_3)_4]Cl_2$ solution containing 2 mg Pt/mL for the purpose of ion exchange. Meanwhile, 1 mL of ammonium hydroxide (NH_4OH) solution (5 wt%) was added to the ion exchange solution. The membrane was kept in the solution at ambient condition for 3-4 days to complete ion exchange from H^+ to Pt^{2+}. After rinsing with DI water, the membrane was placed in water with stirring at 40 °C. Then, 3 mL of sodium borohydride ($NaBH_4$) solution (5 wt%) was added every 30 min for 10 times. During this sequence of addition, the temperature was raised to 60 °C gradually. After 5 h,

20 mL of the reducing agent ($NaBH_4$ solution, 5 wt%) was added to the solution in order to ensure the complete reduction of Pt inside the membranes. Gentle stirring was kept for 2 h at 60 °C. After finishing the primary reduction, the membrane was removed, rinsed with DI water and then soaked in HCl solution (1 M) at 40 °C for 5 h. The membrane was rinsed with a large quantity of DI water several times until the filtrate was neutral. At the beginning of secondary plating, the membrane was placed in 240 mL of stirring $[Pt(NH_3)_4]Cl_2$ solution (0.5 mg Pt/mL) at 40 °C, and 5 mL of NH_4OH solution (5 wt%) was then added. 6 mL of hydrazine hydrate (NH_2NH_2) solution (20 wt%) and 3 mL of hydroxylammonium chloride ($NH_2OH{\cdot}HCl$, 5 wt%) solution was dropped into the Pt solution every 30 min, respectively. The temperature was increased gradually from 40 °C to 60 °C over 4 h. The resulting membrane covered with Pt layers was washed with DI water and immersed in HCl solution (1 M). The plating process was repeated in order to obtain high conductive surfaces, with 3 times of primary plating and 1 time of secondary plating. Because the hydrated IPMC actuator in Li^+ form can show better electromechanical performance,[8] IPMC actuators were soaked in lithium hydroxide (LiOH) solution (1 M) overnight for cation exchange from H^+ to Li^+, then rinsed repeatedly with DI water to remove excessive LiOH, and finally stored in fresh DI water. In addition, Nafion 117-based IPMC actuators were also prepared via the same chemical plating process as mentioned above.

Measurements

Fourier transform infrared spectroscopy (FTIR) spectra were recorded on an Equinox 55 spectrometer (Bruker) in the range of 4000-400 cm^{-1}. The samples were prepared by casting several drops of polymer solutions (2 wt%) onto KBr pellets and dried in oven. ^1H nuclear magnetic resonance (^1H NMR) spectra were performed by a Bruker AV400 NMR spectrometer with deuterated dimethyl sulfoxide (DMSO-d_6) as the solvent and tetramethylsilane (TMS) as the standard.

The thermal stability of the samples was characterized by thermogravimetric analysis (TGA, TGA-7, Perkin-Elmer, USA) at a heating rate of 20 °C min^{-1} in an argon flow (20 mL min^{-1}).

The degree of sulfonation (DS), which is the average number of sulfonic acid groups (SO_3H) per repeating unit in a polymer, can be used to calculate the ion exchange capacity (IEC, meq g^{-1}). The DS and IEC of the membrane were determined by the back-titration method. Firstly, the membrane was converted from the acid form (H^+) to the sodium form (Na^+) by soaking in NaCl aqueous solution (1 M) for 2-3 days. Then, the exchanged proton (H^+) of the solution was titrated with a sodium hydroxide (NaOH) standard solution (25 mM) using phenolphthalein as an indicator. Since IEC is defined as the number of moles of proton per gram of dry polymer, the values of DS and IEC were calculated by the following equations, respectively:

$$DS = \frac{400 \times (\frac{V_{NaOH} \times M_{NaOH}}{W_d})}{1000 - 80 \times (\frac{V_{NaOH} \times M_{NaOH}}{W_d})} \times 100\% \quad (1)$$

$$IEC = \frac{V_{NaOH} \times M_{NaOH}}{W_d} \quad (2)$$

where W_d is the weight (g) of the dry polymer film, and V_{NaOH} and M_{NaOH} represent the consumed NaOH volume (L) and the molarity (mol L^{-1}) of NaOH solution, respectively. The molar masses of the repeating unit of PPSU main chain and the SO_3 group are 400 and 80, respectively.

The water uptake (WU) of the membrane is the weight ratio of absorbed water inside the wet membrane to that of the dry membrane. The WU value was calculated using the equation shown below:

$$WU = \frac{W_{wet} - W_{dry}}{W_{dry}} \quad (3)$$

where W_{wet} and W_{dry} denote the weights of the wet and the dried membranes, respectively.

Proton conductivities (σ) of the full hydrated membranes in the acid form were measured at room temperature by the two-electrode alternating current (AC) impedance method (Autolab PGSTAT302N, Switzerland). The measured process was carried out over a frequency range of 10-10^6 Hz under oscillating voltage of 10 mV. The proton conductivity of membrane was calculated by the following equation:

$$\sigma = \frac{l}{R \cdot w \cdot d} \quad (4)$$

where R, l, w and d are the resistance of the impedance, the distance between the two measured electrodes, the width of the membrane, and the thickness of the hydrated membrane, respectively.

Young's modulus (tensile modulus) and the tensile strength of the dry and the wet membranes were determined by an electric universal testing machine (CMT-4104, Shenzhen Sans Testing Machine Co., Ltd., China). The test was conducted at the tensile speed of 5 mm/min with a 30 mm gauge length. All data were averaged for at least seven samples.

Electrical resistances of the IPMCs along the surface direction of metallic electrodes, namely surface resistances, were measured by the four-probe DC current method using a Keithley 2400 SourceMeter and an Agilent 34401A Digital Multimeter.

The surface and cross-sectional morphologies of IMPC were observed by a field emission scanning electron microscopy (FE-SEM, Sirion 200, FEI Corp., Netherlands). The cross-sectional distribution of platinum element was analyzed using an energy dispersive X-ray spectrometer (EDX, EADX Inc., USA).

For electromechanical tests, the SPPSU-based IPMC were cut into a strip with a width of 5 mm and a length of 40 mm. The IPMC strip was vertically suspended in air, and the top end of the strip was fixed with a electric clamp, while the bottom end remained free with the ability of bending horizontally under the voltage stimulus. In other words, the IPMC strip was in a cantilever configuration. The experimental setup consisted of a laser displacement sensor (LK-G80, Keyence, Japan), a data acquisition system (NI PCIe-6351, National Instruments, USA) and a desktop computer. A current amplifier based on an OPA548 chip (Texas Instruments, USA) was used to supply sufficient electric power for IPMC actuation measurement. The displacement was measured in air at a point which is 25-30 mm away from the fixed end or 5 mm from the free end of a cantilever type of IPMC strip. The displacement was calculated and normalized for different-size IPMC strips under the voltage excitation according to the following equations:[34,52]

$$\delta = (\delta_{max} - \delta_{min}) / 2 \quad (5)$$

$$\varepsilon = \frac{2\delta t}{L_f^2 + \delta^2} \quad (6)$$

where δ_{max} and δ_{min} are the maximum and minimum values of displacement under AC voltage, respectively; ε is the normalized strain, δ is the displacement under DC excitation or the average displacement under AC excitation, t is the thickness of IPMC strip, and L_f is the free length of the sample which is the distance between the measured point and the electrically-clamped fixed end of IPMC strips.

Results and discussion

Chemical structures of PPSU and SPPSU

The polyphenylsulfone (PPSU) is a thermoplastic and hydrophobic polymer with aromatic hydrocarbon (non-fluorinated) backbone. To obtain ionic conductivity, the PPSU was subjected to a sulfonation reaction via electrophilic aromatic substitution. The chemical structures of PPSU and SPPSU, and the sulfonation reaction scheme were shown in Fig. 1. The sulfonic acid group is grafted on high electron density site which is one of four unsubstituted positions (site "a") of the benzene rings between two ether links.

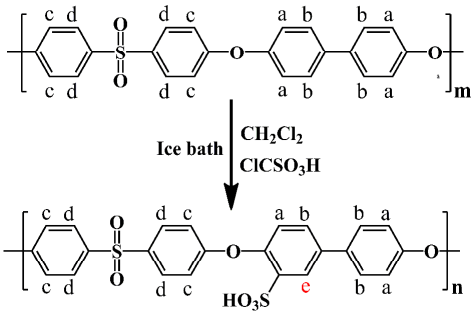

Fig. 1 Synthetic scheme of SPPSU.

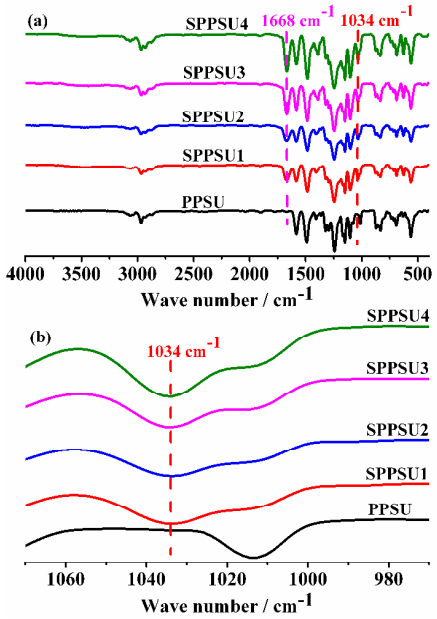

Fig. 2 FTIR spectra of PPSU and SPPSU: the full spectra (a), and local zoom-in view (b).

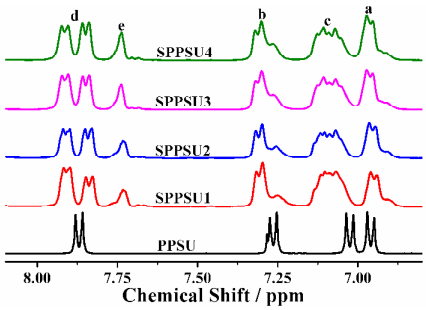

Fig. 3 ^{1}H NMR spectra of PPSU and SPPSU.

To confirm the successful introduction of sulfonic acid group and check the change of chemical structure before and after the sulfonation reaction, FTIR spectroscopy measurement was conducted on the SPPSU polymer. As shown in Fig. 2, the characteristic absorption peaks of sulfonic acid groups (-SO_3H) appear at 1034 cm^{-1}.[53] It is also noted that the absorption intensity of this band increases with the corresponding IEC value increasing. Additionally, another notable difference before and after sulfonation is the presence of a new absorbance peak for SPPSU at 1668 cm^{-1}, which is assigned to one of the peaks associating with the stretching vibration of benzene rings. The intensity of the peaks at 1668 cm^{-1} increases when the amount of substituted polar groups (*i.e.* SO_3H) or the polarity of substituted groups on the benzene rings increases.

^{1}H NMR spectra of PPSU and SPPSU are given in Fig. 3. A new significant signal at 7.74 ppm appears in SPPSU, which is related to the aromatic proton (H_e) *ortho* to -SO_3H at the position e in Fig. 1.[49] It is clear that the intensity (integral area) ratio of H_e signal to that of other aromatic protons is intimately linked to the DS of SPPSU. The ratio increases with increasing of the DS or IEC. Obviously, the result of ^{1}H NMR measurement also confirms that the PPSU polymer is successfully sulfonated.

Thermal analysis

The thermal stabilities of PPSU and SPPSU were examined by TGA under N_2 atmosphere. The pristine PPSU exhibits higher thermal stability than SPPSU (Fig. 4). SPPSU has three stages of weight loss. The initial weight loss occurs at the temperature of 70-200 °C, which corresponds to evaporation of water molecules bonded to the sulfonic groups in SPPSU. The second weight loss occurs in the range of 260-430 °C, which is assigned to the decomposition of sulfonic acid groups (side chains) in SPPSU. Similar to the pristine PPSU, the final weight loss above 560 °C for SPPSU is also ascribed to the degradation of the polymer backbone.

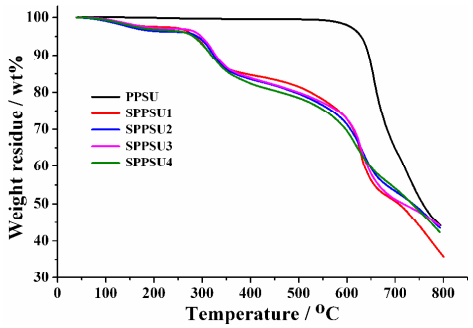

Fig. 4 TGA cures of PPSU and SPPSU.

Table 1 Properties of SPPSU and Nafion membranes

Entry	Sample	IEC (meq g^{-1})	WU (wt%)	σ (S cm^{-1})	Tensile modulus (MPa)		Tensile strength (MPa)	
					dry	wet	dry	wet
1	SPPSU1	1.93	43.5	0.050	1094.7	450.7	52.2	16.4
2	SPPSU2	2.06	49.0	0.068	874.5	422.5	35.3	16.4
3	SPPSU3	2.10	53.8	0.070	863.0	334.9	34.6	12.9
4	SPPSU4	2.23	67.2	0.074	1114.4	296.4	49.7	10.8
5	Nafion 117	1.02	18.7	0.081	174.8	91.6	30.3	20.4

Properties of SPPSU membranes and SPPSU-based IPMCs

The chemical and mechanical properties of SPPSU and Nafion membranes are summarized in Table 1. As expected, the ion exchange capacity (IEC), the water uptake (WU) and the proton conductivity of SPPSU membranes increase with increasing the DS. Moreover, these SPPSU membranes have higher IEC and WU than those of Nafion 117 membrane. The SPPSU4 membrane has the highest IEC of 2.23 meq g^{-1} and WU of 67.2 wt% (entry 4). However, its proton conductivity is 0.074 S cm^{-1}, which is slightly lower than 0.081 S cm^{-1} of the Nafion membrane (entry 5) due to the confinement of SPPSU's higher molecular rigidity, lower aggregation density of short and rigid ionic side chains (sulfonic groups).[39] In Nafion membrane, the long and flexible side chains with the ionic groups at the end, can aggregate and further form well-defined and ionic-nanochannel-connected ionic clusters by microphase separation, which facilitate ion transport along ion channels in Nafion membrane.[54] The high molecular rigidity of the SPPSU membranes leads to higher tensile moduli in dry and wet states relative to the Nafion membranes. Specifically, the tensile modulus and strength of dry SPPSU membranes firstly decreases, and then increases with the corresponding DS increasing. It can be explained that, on the one hand, the introduction of side chains (SO_3H) damages the regularity of arrangement of molecular chain in the solid state;[55] but on the other hand, the introduction increases the interaction between SPPSU molecular chains by hydrogen bonds and polar dipole-dipole interaction. There is a tradeoff between these two effects. However, both the tensile modulus and strength of the membranes in the wet state continuously decrease with increasing the DS or IEC value. This is because absorbed water (WU), of which the amount increases accordingly as the DS or IEC value increases, acts as plasticizer to decrease the interaction between SPPSU segmental chains.[8,9,14,56,57] Although the tensile strength of each hydrated SPPSU membrane is lower than that of Nafion 117 membrane, the hydrated SPPSU membranes show several times higher modulus than that of Nafion membrane. With these improved excellent ion conduction and mechanical properties, SPPSU4 membranes could be a better option for producing high-performance IPMC actuators.

Surface resistance, which can produced a voltage drop along the surface-electrode direction and decrease the actual voltage at the free end of IPMCs, is one of important factors to affect the performance of IPMC actuators.[58] As listed in Table 2, the surface resistances of all IPMC's electrodes are relatively small (below 3.6 Ω sq^{-1}) so that the measured voltage drop at the free end of IPMC strips is not beyond 0.1 V under 1.5 V of applied DC voltages. Therefore, on the whole, the surface resistance of IPMCs is acceptable and more or less approximative. The mechanical properties of SPPSU-based and Nafion-based IPMCs were also investigated and summarized in Table 2. Similar to pure SPPSU membranes, the tensile modulus and strength of SPPSU-based IPMCs in the wet state decrease with increasing the DS or IEC value of the corresponding SPPSU membrane. However, there are still some differences in mechanical properties between the SPPSU-based IPMCs and pure SPPSU membranes, which are mainly ascribed to the competing influences from three aspects induced by the chemical plating process. Specifically, the first kind of influence results from the pretreatment before chemical plating (rubbing the surfaces of SPPSU membranes by the sandpapers), which produces some cracks or mechanical defects on the the surfaces of SPPSU membranes; thus, it will decrease the mechanical properties (tensile modulus and strength) of SPPSU membranes and subsequent IPMCs. The second kind of influence is from further swelling or more absorbed water of SPPSU membranes when they undergo higher temperature (40-60 ^{o}C) than room temperature in the water within the chemical plating process, which will further decrease the mechanical properties of SPPSU membranes and subsequent IPMCs. On the contrary, the third kind of influence can increase the mechanical properties due to the enhancing effect of coating metallic electrodes. As a result, compared to wet pure SPPSU or Nafion membranes, the corresponding IPMCs in wet state don't show significant advantages in terms of mechanical properties; even in most case, the mechanical properties of IPMCs are inferior to those of pure SPPSU or Nafion membranes. In addition, after 3-min actuation in the air under the sinusoidal voltage of 3V and 1Hz, the tensile modulus and strength of IPMCs become slightly lower perhaps due to somewhat destroying of surface electrodes of the IPMCs during the repeatedly-bending-deformation cycle.

Table 2 Properties of SPPSU-based and Nafion-based IPMCs in wet state

Entry	Sample	Surface resistance (Ω sq^{-1})	Tensile modulus (MPa)		Tensile strength (MPa)	
			before actuation	after 3-min actuation	before actuation	after 3-min actuation
1	SPPSU1-based IPMC	2.35	604.9	541.7	15.9	14.3
2	SPPSU2-based IPMC	0.87	392.8	367.7	8.8	8.7
3	SPPSU3-based IPMC	3.50	358.7	325.7	8.8	8.4
4	SPPSU4-based IPMC	2.01	272.2	260.8	7.5	6.9
5	Nafion-based IPMC	3.55	110.6	101.5	11.8	11.6

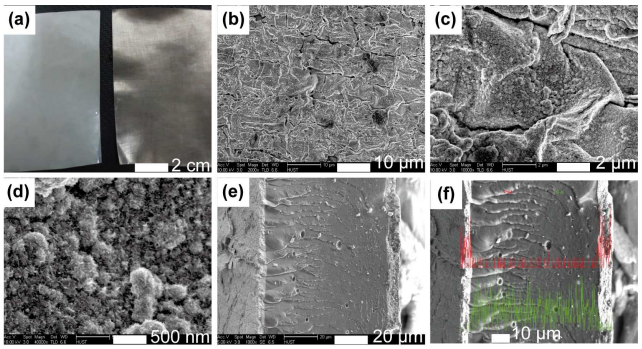

Fig. 5 Optical photograph of pure SPPSU4 membrane (left) and platinum-plated SPPSU4-based IPMC (a); SEM micrographs of the surface (b)-(d) and cross-section (e)-(f) of SPPSU4-based IPMC. The red line in Fig. 5f represents EDX line-scan analysis for Pt along the cross section of the SPPSU4-based IPMC actuator.

Morphology of SPPSU4-based IPMC

The surface and cross-sectional morphologies of the SPPSU4-based IPMC actuator are shown in Fig. 5. It is clearly observed from Fig. 5a that there is a metallic luster on the SPPSU membrane after chemical plating of platinum (Pt). As shown in Figs. 5b and 5c, Pt particles are densely deposited on the electrode surface of the IPMC actuator. Besides, some microcracks are observed on the Pt electrode layers of SPPSU4-based actuator as a result of the cracking of the Pt electrode layers during the sample drying process before SEM measurement.[34] Fig. 5d reveals that there are many small dendritic Pt nanoparticles on the top Pt electrode layers, and these Pt nanoparticles are interconnected and densely coagulated, which contributes to improve the conductivity of the IPMC electrodes. As is clearly seen in Fig. 5e, two layers of thick Pt electrodes of about 5-8 μm thickness are coated on both the sides of SPPSU4 membrane. In addition, the EDX characterization exhibits that the Pt particles are not homogeneously distributed through the cross-section of SPPSU4 membrane (Fig. 5f), but the Pt particles predominantly deposit near the interface boundaries of SPPSU4 membrane, forming the Pt particle surface layers. Besides, some Pt particles deeply diffuse into the SPPSU4 membrane, and the density of Pt particles decreases toward the middle part of the SPPSU4 membrane. The Pt diffusion layers can enhance the interfacial adhesion between the electrode and membrane in this IPMC.

Actuation performance of the SPPSU-based IPMC actuators

The SPPSU-based IPMC actuators were measured to obtain tip displacement and normalized bending strain under DC and sinusoidal voltages in air, respectively.

Fig. 6a shows the time-bending strain curves of the four kinds of SPPSU-based IPMC actuators and Nafion-based IPMC actuator under an applied DC voltage of 3 V. When the DC voltage is applied across the thickness of the water-saturated SPPSU-based IPMCs in the cantilever configuration, these actuators immediately bend toward the anode side. The bending deformation is believed to be originated from the combined effects of the electrophoretic migration of hydrated Li cations, and subsequent electro-osmosis drag of free water molecules toward the cathode, which produce water-concentration-gradient-induced differential or asymmetric swelling on the two sides of IPMC strip (in details: expansion of the cathode side *vs.* contraction of the anode side).[4] Among the prepared four kinds of SPPSU-based IPMC actuators, the SPPSU4-based IPMC performs the best actuation performance, and shows the largest max. bending strain (MBS) of 3,760 × 10^{-6} within 500 ms under a DC voltage of 3 V, which is ascribed to its highest IEC, water uptake, ionic conductivity and lowest hydrated tensile modulus (Table 1). Higher IEC, which means larger number of sulfonic groups and more available mobile cations as well as higher adsorbed water for polymer electrolyte membrane, thereby results in larger volume of water moving toward the cathode by the action of hydrated cation electrophoresis and electro-osmosis drag of water, greater volume expansion on the cathode side and consequent larger bending deformation.[13,15,37] In addition, under the premise of guaranteed dimensional stability, low mechanical modulus is helpful for the realization of large bending displacement.[41,42] This is because the resistant force against deformation, produced by the IPMC cantilever beam itself,[25] decreases along with decreasing mechanical modulus of IPMC; consequently, the hydraulic actuation force generated in hydrated IPMCs under the electric excitation can more easily overcome the anti-deformation force of the IPMC beam with lower hydrated modulus. Compared with the Nafion-based IPMC actuator under the identical DC voltage of 3 V, the SPPSU4-based IPMC shows comparable or slightly lower MBS than that of the Nafion counterpart (*i.e.* 3,960 × 10^{-6}). However, similar to Nafion-based IPMC actuator, all four SPPSU-based actuators show obvious back-relaxation phenomenon. Back-relaxation by an IPMC actuator refers to a phenomenon in which the actuator cannot maintain the maximum bending deformation and return toward the initial (zero) position in the opposite direction immediately after it reaches its largest deformation under a sustained constant DC voltage. The back-relaxation of the bending strain in IPMCs

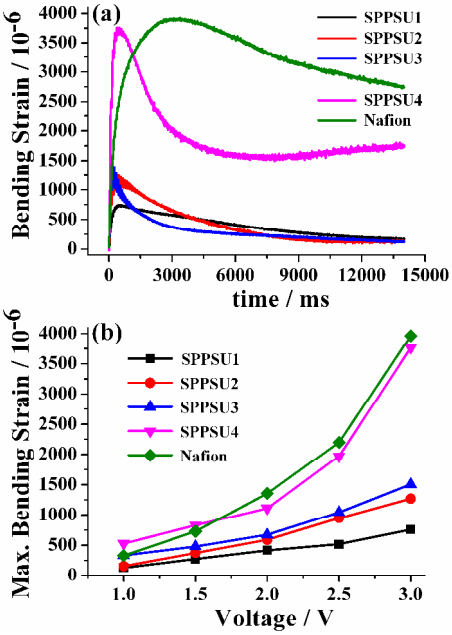

Fig. 6 Bending strain as a function of time for various SPPSU-based IPMC actuators in air under DC voltage of 3 V (a); voltage dependence of maximum bending strain of various SPPSU-based IPMC actuators (b).

may be caused by the diffusing back of water toward the anode side as a result of concentration gradient and pressure gradient of water.[13,24,34] This process of relaxation will be terminated when a new equilibrium of water is established. Another interesting feature observed in Fig. 6a is that all the SPPSU-based actuators need much shorter time for attaining the MBS compared to the Nafion one. Although the MBS of SPPSU4 actuator is comparable to that of Nafion counterpart, the response time for maximum strain is greatly reduced to 486 ms for SSPSU4 actuator, compared with 3,250 ms for Nafion actuator. Moreover, the response times of all SPPSU-based actuators are less than 600 ms, and three other SPPSU actuators except for SPPSU4 one exhibit the decreasing trend in the response time as the IEC of the corresponding SPPSU membrane increases, which is attributed to the increase of their number of movable hydrated cation, amount of migrating water and ion conductivity together with the decrease of hydrated mechanical modulus. The voltage-dependent max. strains of the SPPSU actuators and the Nafion actuator are shown in Fig. 6b. The MBS of all the actuators gradually increases as the amplitude of the applied DC voltage increases, which complies with the general characteristics of IPMC actuator. The electrophoresis and electro-osmosis originate from the application of the voltage through the IPMC. Consequently, higher voltage can produce more accumulation of hydrated cation and water near the cathode boundary, greater volume expansion at the cathode side, and a larger bending strain as a result.[59] Moreover, the SPPSU4 and Nafion actuators show significantly lager bending strain relative to other SPPSU actuators, especially when the voltage exceeds 2 V. The SPPSU4 actuator has a comparable value of max. strain as that of Nafion counterpart, which is perhaps due to their approximately identical ion conductivity, as well as good compromise between the positive effect of IEC and water uptake and the negative effect of hydrated mechanical modulus on the electromechanical performance of IPMC actuator. It is also noted that the max. strain of the SPPSU actuator always increase in the order of SPPSU1 < SPPSU2 < SPPSU3 < SPPSU4, regardless of the amplitude of input DC voltage. Meanwhile, the SPPSU2 actuator and SPPSU3 actuator display more or less the same electromechanical performance in terms of MBS, which can be explained by their approximate physical properties.

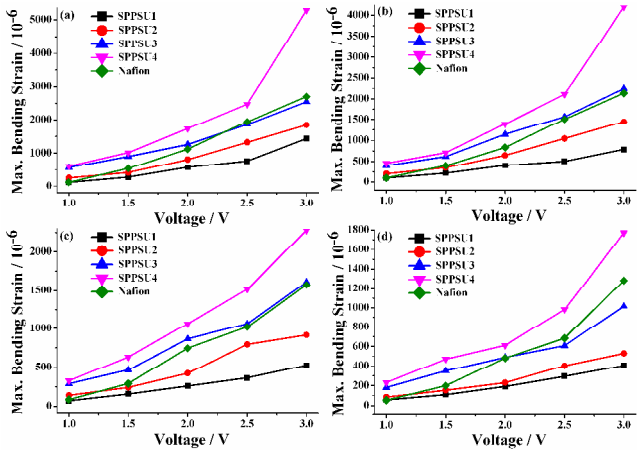

Fig. 7 Voltage-dependent maximum bending strain for various SPPSU-based IPMC actuators and Nafion actuator at 1 Hz (a), 2 Hz (b), 5 Hz (c) and 10 Hz (d), respectively.

Fig. 7 shows the dependence of MBS on the amplitude of voltage for IPMC actuators under the sinusoidal excitation. It can be seen that the MBS of all actuators is relatively small under low voltage below 1.5 V. There is a great improvement once the applied sinusoidal voltage exceeds 1.5 V. In addition, the max. strain of IPMC actuator increases accordingly with increasing the sinusoidal voltage, which is consistent with the general law of the traditional IPMC actuator. The MBS of these SPPSU-based IPMC actuators follows the order of SPPSU4 > SPPSU3 > SPPSU2 > SPPSU1. It should also be highlighted that, under the same experimental conditions, the SPPSU4-based IPMC actuator shows superior bending performance to that the Nafion-based system. Even, most of the time, the MBS of SPPSU3 actuator is more than that of the Nafion counterpart. At high voltage beyond 2 V, the actuation performance of Nafion actuator begins to approximate (*i.e.* at the frequency of less than 10 Hz) or surpass (*i.e.* at 10 Hz) that of SPPSU3 actuator. These exciting results are anticipated from the previously shown advantages of SPPSU3 and SPPSU4 membranes over Nafion counterpart in terms of higher IEC, higher WU, and slightly lower ion conductivity.

Also, all the as-prepared IPMC actuators show an obvious dependence on the frequency of electric voltage. As shown in Fig. 8, these IPMC actuators show large MBS at low frequency of 1 Hz. With increasing the frequency, their MBS decreases rapidly. As the frequency is up to 5 Hz, the decreasing trend begins to become slow. The principle of actuation for IPMC actuator is thought to be ion flux and electro-osmotic drag of water toward the cathode side, and therefore, the dependence of the MBS on electric frequency is closely related to the speed and total time of migration and accumulation of cations and water. At lower frequency, there is relatively sufficient time for migration and accumulation of cations and water in IPMC actuators, which leads to larger bending strain. Whereas at higher frequency, the speed of movement of cations and water is much slower than the converting speed of the voltage polarity. Consequently, the cations and water have insufficient time to migrate and accumulate toward the transient cathode, which results in the smaller bending strain of IPMC actuators.[42,43,58] Similar to the above-mentioned observation, in Fig. 8f, the SPPSU4 actuator also shows the largest bending strain for all frequencies at 3 V, and even the maximum bending strain of SPPSU3 actuator is more or less the same as that of Nafion counterpart at 3 V peak voltage.

As mentioned above, all the IPMC actuators show their best electromechanical performance under sinusoidal excitation of 3 V at 1 Hz, thereby it is essential to check and compare their bending response with time in such case. Clearly seen from Fig. 9b, the SPPSU4 actuator shows the best bending performance and prevails over other actuators. The max. strain of SPPSU4 actuator is approximately twice as much as that of Nafion actuator under 3 V sinusoidal voltage at 1 Hz. This is a very great improvement and demonstrates that SPPSU4 is a good candidate to replace Nafion for the purpose of preparing high-performance IPMC actuator.

To further explore the harmonic actuation response of the best performer (SPPSU4 actuator), the measured bending strain for the SPPSU4-based IPMC actuator under sinusoidal electric stimulation of 3 V at different frequencies, and sinusoidal electric

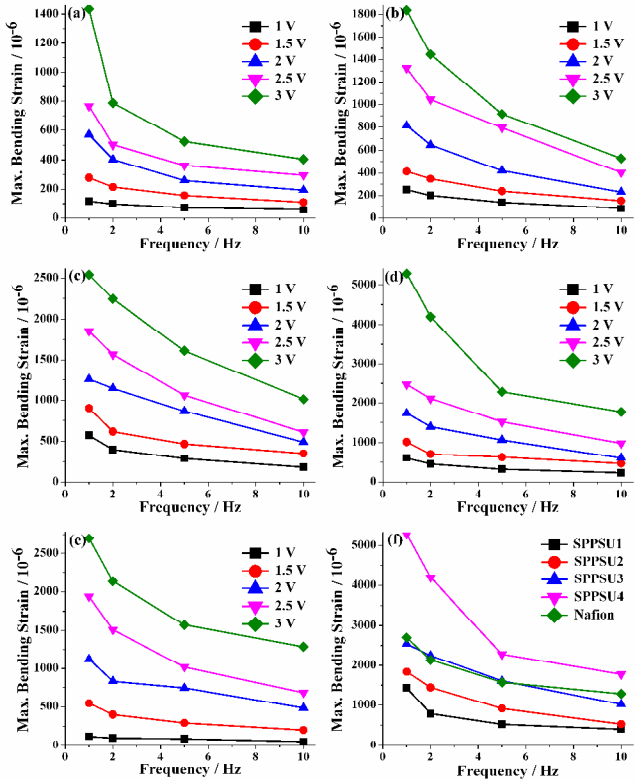

Fig. 8 Maximum bending strain vs. frequency curves under sinusoidal voltage with different amplitudes, respectively for SPPSU1-based IPMC actuator (a), SPPSU2-based IPMC actuator (b), SPPSU3-based IPMC actuator (c), and SPPSU4-based IPMC actuator (d), Nafion-based actuator (e) and comparison of various actuators under sinusoidal voltage with 3 V peak (f).

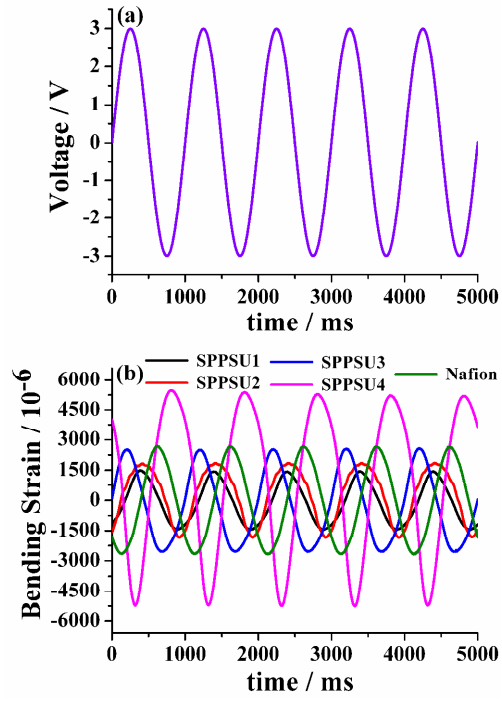

Fig. 9 Time-voltage curve (a), and Harmonic bending response of various SPPSU actuators and Nafion actuator (b) under the sinusoidal voltage with the amplitude of 3 V at the frequency of 1 Hz.

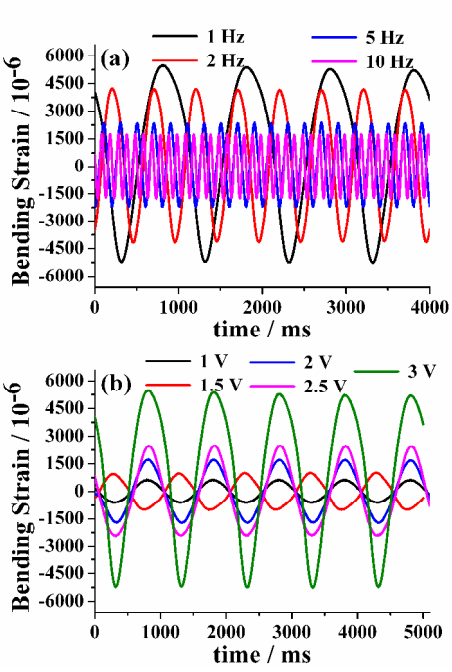

Fig. 10 Comparison of bending strain for SPPSU4-based IPMC actuators under sinusoidal excitation of 3 V at different frequencies (a); sinusoidal electric stimulation at 1 Hz with different voltages (b).

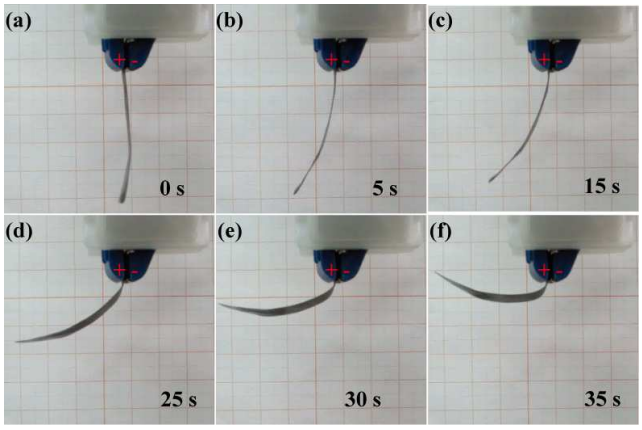

Fig. 11 Successive photographs of SPPSU4-based IPMC actuator recorded by a digital camera at different times under DC voltage of 3 V.

frequency of 1 Hz at different voltage, is shown and compared in Figs. 10a and 10b, respectively. As observed, the MBS of SPPSU4 actuator increases along with decreasing the frequency of the input sinusoidal voltage and increasing the peak voltage. Besides, under sustaining sinusoidal electric stimulation, the bending strain of the SPPSU4-based IPMC actuator does not decrease obviously with time, and the time-strain response is harmonic without a severe distortion. These are intimately related to good quality of electrodes and strong interfacial adhesion between the electrode and membrane for SPPSU4 actuator.

In order to more intuitively observe and truly demonstrate the bending deformation of SPPSU actuators, a series of photographs were captured by a commercial digital camera at different times during actuation process of SPPSU4 actuator (see Fig. 11). Prior to photographing, an essential pretreatment should be carried out to decrease the speed of bending response of SPPSU4 IPMC actuator under DC voltage, and assure a real-time recording of

bending deformation by a camera. A filter paper was used to wipe off trace water on the electrode surface of SPPSU4 actuator for two purposes of increasing the stiffness of electrode layers and reducing the total amount of absorbed water in the IPMC actuator. Fig. 11 shows six successive photographs of SPPSU4 actuator under DC voltage of 3 V after the pretreatment. As can clearly seen, the cantilevered strip of SPPSU4 actuator bends toward the anode side after the application of DC voltage. With the time increasing, the degree of bending deformation increases continuously. When the applied time of sustained DC voltage reachs 35 seconds, the bending angle of the SPPSU4 actuator exceeds 90°.

Conclusions

Four kinds of sulfonated polyphenylsulfone (SPPSU) with different degree of sulfonation (DS) or ion exchange capacity (IEC) were synthesized, and their IPMC actuators based SPPSU membranes were successfully prepared through the solution-casting method and consecutive electroless plating procedure. Experimental results demonstrated the DS or IEC was one of dominant factors determining the property of SPPSU ion exchange membrane, thereby largely affected the electromechanical performance of SPPSU IPMC actuators. With the increase of DS of SPPSU membrane, the IEC, water uptake and ion conductivity of corresponding membrane increase, whereas the hydrated mechanical strength and modulus decrease accordingly. These improved properties synergistically contribute to the dramatically enhanced bending performance of SPPSU actuators. Compared with Nafion 117 membrane, in spite of having higher hydrated mechanical modulus, the SPPSU4 membrane with the highest DS (108.7%) shows almost twice IEC, 3.5 times water uptake and slightly lower ion conductivity as much as those of Nafion counterpart, respectively. Among four SPPSU actuators, the SPPSU4 IPMC actuator shows the largest max. bending strain under the DC and sinusoidal voltages. In the case of DC excitation, the SPPSU4 actuator gives more rapid bending response relative to Nafion actuator, and its max. strain is comparable to that of Nafion counterpart at DC voltage of 3 V. More incredibly, the max. strain of SPPSU4 actuator is approximately twice as much as that of Nafion actuator under 3 V sinusoidal voltage at 1 Hz. This is a very great improvement and demonstrates that cost-effective and property-adjustable SPPSU is a promising electroactive polymer which can serve as an alternative of Nafion used in the field of soft actuators, soft sensors and artificial muscles.

Acknowledgements

This work was financially supported by the National Basic Research Program of China (973 Program, 2012CB025903), and National Natural Science Foundation of China (51210004, 50873040). The authors also gratefully acknowledged the Analytical and Testing Center of Huazhong University of Science and Technology for use of measurement facilities.

Notes and references

Key Laboratory for Large-Format Battery Materials and Systems, Ministry of Education, School of Chemistry and Chemical Engineering, Huazhong University of Science and Technology, Wuhan 430074, China. Fax: +86 27 87543632; Tel: +86 27 87793241; E-mail: zgxue@mail.hust.edu.cn; xlxie@mail.hust.edu.cn

1. Y. Bar-Cohen, *Electroactive Polymer (EAP) Actuators as Artificial Muscles: Reality, Potential, and Challenges*, SPIE Press, Washington, 2004.
2. K. J. Kim and S. Tadokoro, *Electroactive polymers for robotics applications: artificial muscles and sensors*, Springer, London, 2007.
3. F. Carpi and E. Smela, *Biomedical Applications of Electroactive Polymer Actuators*, John Wiley & Sons, Ltd, Chichester, 2009.
4. M. Shahinpoor and K. J. Kim, *Smart Mater. Struct.*, 2001, **10**, 819-833.
5. A. J. Duncan, D. J. Leo and T. E. Long, *Macromolecules*, 2008, **41**, 7765-7775.
6. R. Tiwari and E. Garcia, *Smart Mater. Struct.*, 2011, **20**, 083001.
7. C. Jo, D. Pugal, I.-K. Oh, K. J. Kim and K. Asaka, *Prog. Polym. Sci.*, 2013, **38**, 1037-1066.
8. S. Nemat-Nasser and Y. Wu, *J. Appl. Phys.*, 2003, **93**, 5255-5267.
9. S. Nemat-Nasser, S. Zamani and Y. Tor, *J. Appl. Phys.*, 2006, **99**, 104902.
10. S. Nemat-Nasser and Y. Wu, *Smart Mater. Struct.*, 2006, **15**, 909-923.
11. H. M. Jeong, S. M. Woo, H. S. Kim, B. K. Kim, J. H. Bang, S. Lee and M. S. Mun, *Macromol. Res.*, 2004, **12**, 593-597.
12. H. Y. Jeong and B. K. Kim, *J. Appl. Polym. Sci.*, 2006, **99**, 2687-2693.
13. M. J. Han, J. H. Park, J. Y. Lee and J. Y. Jho, *Macromol. Rapid Commun.*, 2006, **27**, 219-222.
14. J. Y. Lee, H. S. Wang, B. R. Yoon, M. J. Han and J. Y. Jho, *Macromol. Rapid Commun.*, 2010, **31**, 1897-1902.
15. J. Y. Lee, H. S. Wang, M. J. Han, G.-C. Cha, S. H. Jung, S. Lee and J. Y. Jho, *Macromol. Res.*, 2011, **19**, 1014-1021.
16. X.-L. Wang, I.-K. Oh, J. Lu, J. Ju and S. Lee, *Mater. Lett.*, 2007, **61**, 5117-5120.
17. X.-L. Wang, I.-K. Oh and J.-B. Kim, *Compos. Sci. Technol.*, 2009, **69**, 2098-2101.
18. P. H. Vargantwar, R. Shankar, A. S. Krishnan, T. K. Ghosh and R. J. Spontak, *Soft Matter*, 2011, **7**, 1651-1655.
19. P. H. Vargantwar, K. E. Roskov, T. K. Ghosh and R. J. Spontak, *Macromol. Rapid Commun.*, 2012, **33**, 61-68.
20. J.-W. Lee, S. M. Hong, J. Kim and C. M. Koo, *Sens. Actuators B: Chem.*, 2012, **162**, 369-376.
21. J.-W. Lee, S. Yu, S. M. Hong and C. M. Koo, *J. Mater. Chem. C*, 2013, **1**, 3784-3793.
22. O. Kim, T. J. Shin and M. J. Park, *Nat. Commun.*, 2013, **4**, 2208.
23. A. K. Phillips and R. B. Moore, *Polymer*, 2005, **46**, 7788-7802.
24. X.-L. Wang, I.-K. Oh and T.-H. Cheng, *Polym. Int.*, 2010, **59**, 305-312.
25. X.-L. Wang, I.-K. Oh and L. Xu, *Sens. Actuators B: Chem.*, 2010, **145**, 635-642.
26. F.-P. Du, C.-Y. Tang, X.-L. Xie, X.-P. Zhou and L. Tan, *J. Phys. Chem. C*, 2009, **113**, 7223-7226.
27. F.-P. Du, C.-Y. Tang, X.-P. Zhou and X.-L. Xie, *J. Compos. Mater.*, 2011, **45**, 2055-2060.
28. K. B. Wiles, B. J. Akle, M. A. Hickner, M. Bennett, D. J. Leo and J. E. McGrath, *J. Electrochem. Soc.*, 2007, **154**, P77-P85.
29. J.-H. Jeon, S.-P. Kang, S. Lee and I.-K. Oh, *Sens. Actuators B: Chem.*, 2009, **143**, 357-364.
30. M. Rajagopalan, J.-H. Jeon and I.-K. Oh, *Sens. Actuators B: Chem.*, 2010, **151**, 198-204.
31. M. Rajagopalan and I.-K. Oh, *ACS Nano*, 2011, **5**, 2248-2256.
32. J. Song, J. H. Jeon, I. K. Oh and K. C. Park, *Macromol. Rapid Commun.*, 2011, **32**, 1583-1587.
33. X.-L. Wang, I.-K. Oh and S. Lee, *Sens. Actuators B: Chem.*, 2010, **150**, 57-64.
34. J. Lu, S.-G. Kim, S. Lee and I.-K. Oh, *Adv. Func. Mater.*, 2008, **18**, 1290-1298.
35. J. Lu, S.-G. Kim, S. Lee and I.-K. Oh, *Smart Mater. Struct.*, 2008, **17**, 045002.

36. J. Lu, S.-G. Kim, S. Lee and I.-K. Oh, *Macromol. Chem. Phys.*, 2011, **212**, 635-642.
37. C.-A. Dai, C.-J. Chang, A.-C. Kao, W.-B. Tsai, W.-S. Chen, W.-M. Liu, W.-P. Shih and C.-C. Ma, *Sens. Actuators A: Phys.*, 2009, **155**, 152-162.
38. C.-A. Dai, C.-C. Hsiao, S.-C. Weng, A.-C. Kao, C.-P. Liu, W.-B. Tsai, W.-S. Chen, W.-M. Liu, W.-P. Shih and C.-C. Ma, *Smart Mater. Struct.*, 2009, **18**, 085016.
39. J.-W. Lee, J.-H. Kim, N. S. Goo, J. Y. Lee and Y.-T. Yoo, *J.Bionic Eng.*, 2010, **7**, 19-28.
40. M. Luqman, J.-W. Lee, K.-K. Moon and Y.-T. Yoo, *J. Ind. Eng. Chem.*, 2011, **17**, 49-55.
41. V. Panwar, K. Cha, J.-O. Park and S. Park, *Sens. Actuators B: Chem.*, 2012, **161**, 460-470.
42. V. Panwar, C. Lee, S. Y. Ko, J.-O. Park and S. Park, *Mater. Chem. Phys.*, 2012, **135**, 928-937.
43. V. Panwar, S. Y. Ko, J.-O. Park and S. Park, *Sens. Actuators B: Chem.*, 2013, **183**, 504-517.
44. J.-H. Jeon, R. K. Cheedarala, C.-D. Kee and I.-K. Oh, *Adv. Func. Mater.*, 2013, **23**, 6007-6018.
45. H. M. Jeong, S. M. Woo, S. Lee, G.-C. Cha and M. S. Mun, *J. Appl. Polym. Sci.*, 2006, **99**, 1732-1739.
46. B. Decker, C. Hartmann-Thompson, P. I. Carver, S. E. Keinath and P. R. Santurri, *Chem. Mater.*, 2010, **22**, 942-948.
47. J.-R. Lee, J.-H. Won, K.-S. Yoon, Y. T. Hong and S.-Y. Lee, *Int. J. Hydrogen Energy*, 2012, **37**, 6182-6188.
48. D. M. Stevens, B. Mickols and C. V. Funk, *J. Membr. Sci.*, 2014, **452**, 193-202.
49. C. Hartmann-Thompson, A. Merrington, P. I. Carver, D. L. Keeley, J. L. Rousseau, D. Hucul, K. J. Bruza, L. S. Thomas, S. E. Keinath, R. M. Nowak, D. M. Katona and P. R. Santurri, *J. Appl. Polym. Sci.*, 2008, **110**, 958-974.
50. M. Yu, H. Shen and Z.-d. Dai, *J. Bionic Eng.*, 2007, **4**, 143-149.
51. Y. Joanne, F. Li Shu, H. Choy Wing, M. Yuen Chun Wah and W. Kan Chi, *Smart Mater. Struct.*, 2011, **20**, 015009.
52. T. Sugino, K. Kiyohara, I. Takeuchi, K. Mukai and K. Asaka, *Sens. Actuators B: Chem.*, 2009, **141**, 179-186.
53. B. C. Johnson, İ. Yilgör, C. Tran, M. Iqbal, J. P. Wightman, D. R. Lloyd and J. E. McGrath, *J. Polym. Sci., Part A: Polym. Chem.,* 1984, **22**, 721-737.
54. K. A. Mauritz and R. B. Moore, *Chem. Rev.*, 2004, **104**, 4535-4585.
55. S. Yang, C. Gong, R. Guan, H. Zou and H. Dai, *Polym. Adv. Technol.*, 2006, **17**, 360-365.
56. P. Genova-Dimitrova, B. Baradie, D. Foscallo, C. Poinsignon and J. Y. Sanchez, *J. Membr. Sci.*, 2001, **185**, 59-71.
57. E. Sgreccia, J. F. Chailan, M. Khadhraoui, M. L. Di Vona and P. Knauth, *J. Power Sources*, 2010, **195**, 7770-7775.
58. M. Shahinpoor and K. J. Kim, *Smart Mater. Struct.*, 2000, **9**, 543-551.
59. L. Naji, J. A. Chudek, E. W. Abel and R. T. Baker, *J. Mater. Chem. B*, 2013, **1**, 2502-2514.

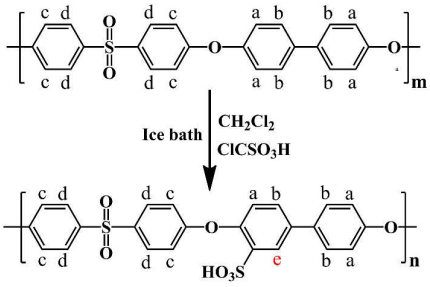

Fig. 1. Synthetic scheme of SPPSU.

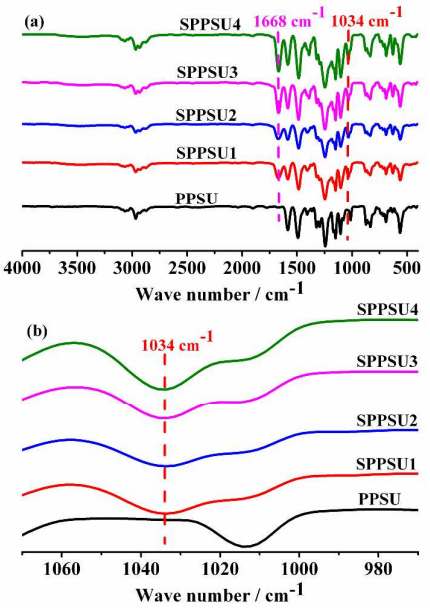

Fig. 2. FTIR spectra of PPSU and SPPSU: the full spectra (a), and local zoom-in view (b).

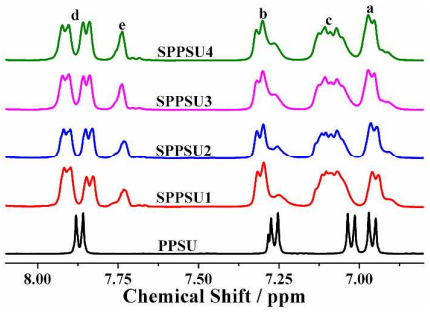

Fig. 3. ^{1}H NMR spectra of PPSU and SPPSU.

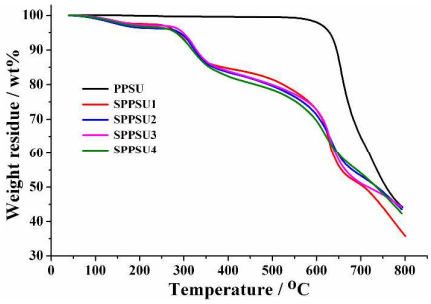

Fig. 4. TGA cures of PPSU and SPPSU.

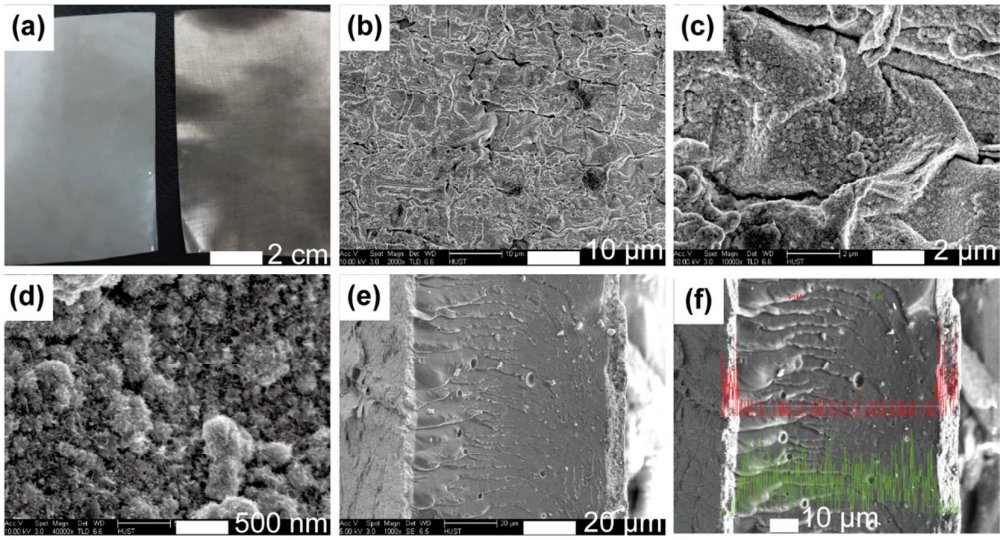

Fig. 5. Optical photograph of pure SPPSU4 membrane (left) and platinum-plated SPPSU4-based IPMC (a); SEM micrographs of the surface (b)-(d) and cross-section (e)-(f) of SPPSU4-based IPMC. The red line in Fig. 5f represents EDX line-scan analysis for Pt along the cross section of the SPPSU4-based IPMC actuator.

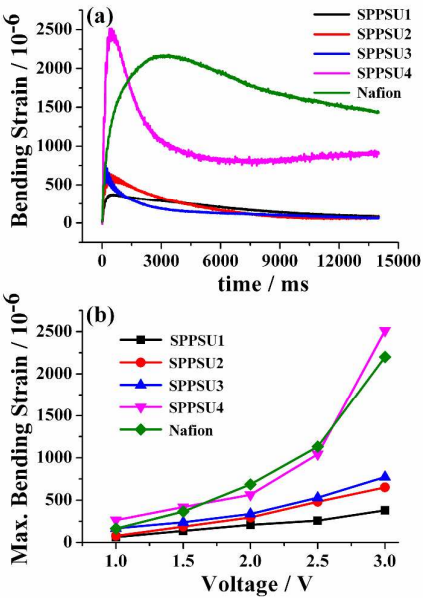

Fig. 6. Bending strain as a function of time for various SPPSU-based IPMC actuators in air under DC voltage of 3 V (a); voltage dependence of maximum bending strain of various SPPSU-based IPMC actuators (b).

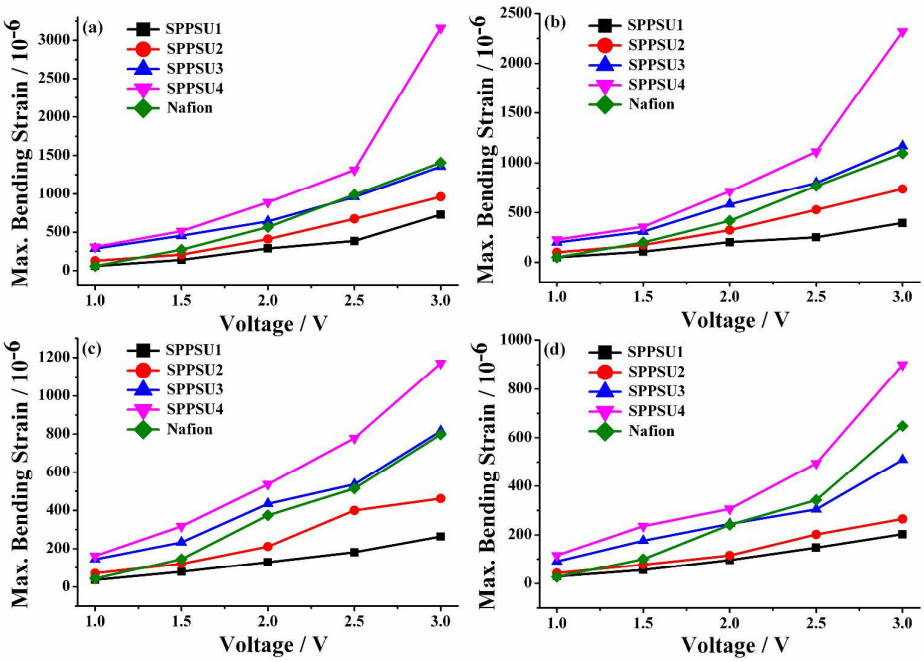

Fig. 7. Voltage-dependent maximum bending strain for various SPPSU-based IPMC actuators and Nafion actuator at 1 Hz (a), 2 Hz (b), 5 Hz (c) and 10 Hz (d), respectively.

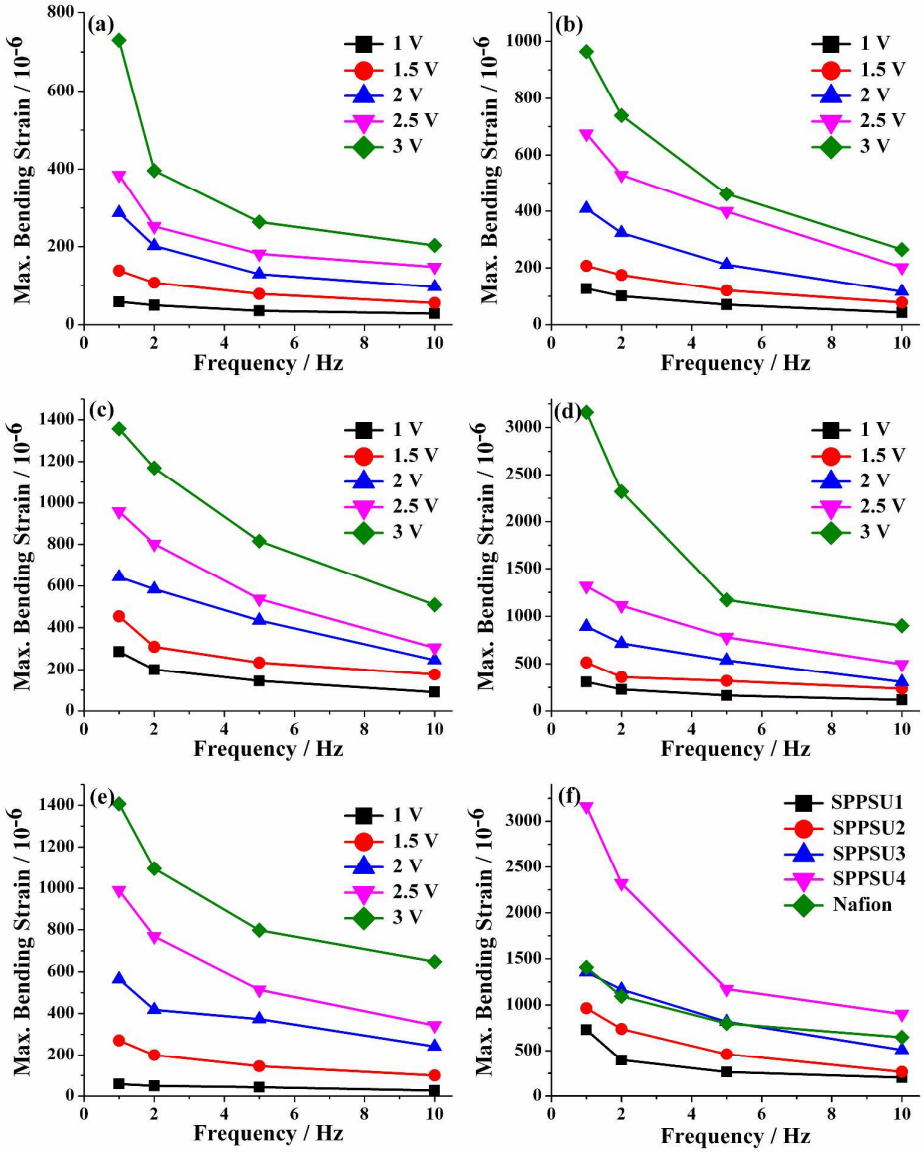

Fig. 8. Maximum bending strain vs. frequency curves under sinusoidal voltage with different amplitudes, respectively for SPPSU1-based IPMC actuator (a), SPPSU2-based IPMC actuator (b), SPPSU3-based IPMC actuator (c), and SPPSU4-based IPMC actuator (d), Nafion-based actuator (e) and comparison of various actuators under sinusoidal voltage with 3 Vpeak (f).

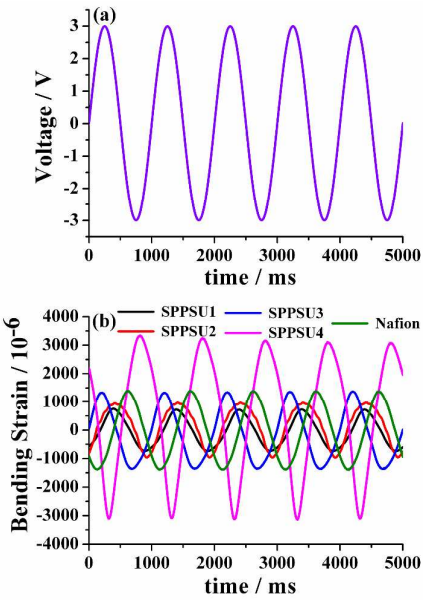

Fig. 9 Time-voltage curve (a), and Harmonic bending response of various SPPSU actuators and Nafion actuator (b) under the sinusoidal voltage with the amplitude of 3 V at the frequency of 1 Hz.

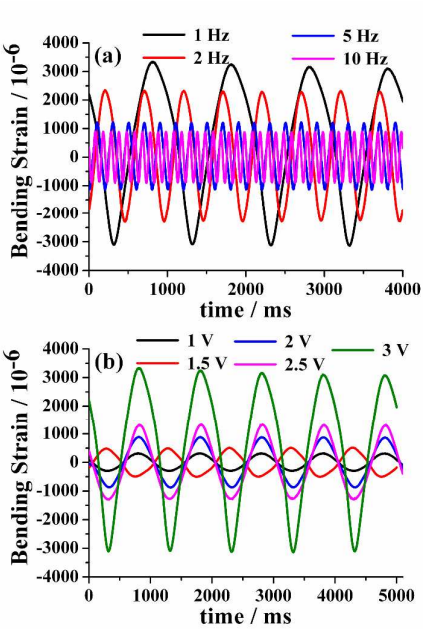

Fig. 10. Comparison of bending strain for SPPSU4-based IPMC actuators under sinusoidal excitation of 3 V at different frequencies (a); sinusoidal electric stimulation at 1 Hz with different voltages (b).

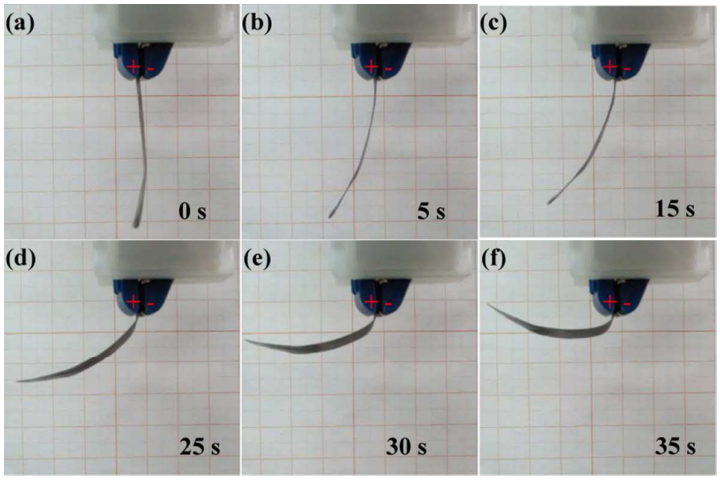

Fig. 11. Successive photographs of SPPSU4-based IPMC actuator recorded by a digital camera at different time under DC voltage of 3 V.

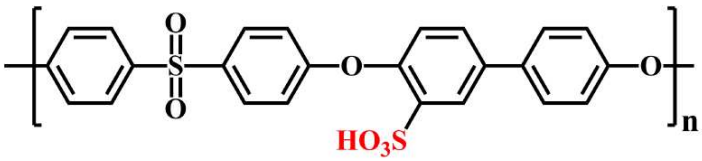

Sulfonated polyphenylsulfone (SPPSU)

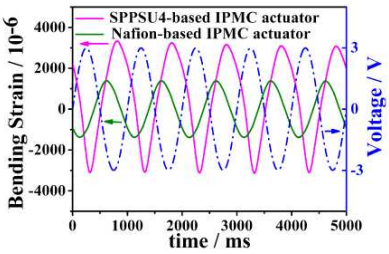

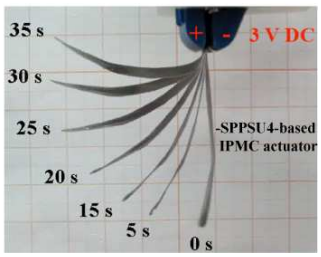

The novel SPPSU-based IPMC membranes with different ion exchange capacities were synthesized. SPPSU4-based IPMCs showed the best actuation performance.